ACS APPLIED MATERIALS & INTERFACES

Research Article

www.acsami.org

Universal Coating from Electrostatic Self-Assembly to Prevent Multidrug-Resistant Bacterial Colonization on Medical Devices and Solid Surfaces

Wenshu Zheng,[†,‡] Yuexiao Jia,[†] Wenwen Chen,[†,⊥] Guanlin Wang,[†] Xuefeng Guo,[‡] and Xingyu Jiang*[,†]

[†]Beijing Engineering Research Center for BioNanotechnology & Key Lab for Biological effects of Nanomaterials and Nanosafety, CAS Center for Excellence in Nanoscience, National Center for NanoScience and Technology & University of the Chinese Academy of Sciences, 11 Beiyitiao, Zhongguancun, Beijing 100190, China

[‡]Academy for Advanced Interdisciplinary Studies, Peking University, Beijing 100871, China

Supporting Information

ABSTRACT: We provide a facile and scalable strategy for preparing gold nanoparticles (AuNPs)-based antibacterial coating on a variety of surfaces through electrostatic self-assembly. AuNPs conjugated with 4,6-diamino-2-pyrimidinethiol (DAPT, not antibacterial by itself), AuDAPT, can form stable coating on different substrates made from polyethylene (PS), polyvinyl chloride (PVC), polypropylene (PP), polyethylene (PE), polydimethylsiloxane (PDMS), and SiO_2 in one step. Such a coating can efficiently eradicate pathogenic Gram-negative bacteria and even multidrug-resistant (MDR) mutants without causing any side-effect such as cytotoxicity, hemolysis, coagulation, and inflammation. We show that immobilized AuDAPT, instead of AuDAPT released from the substrate, is responsible for killing the bacteria and that the antimicrobial components do not enter into the environment to cause secondary contamination to breed drug resistance. Advantages for such coating include applicability on a broad range of surfaces, low cost, stability, high antibacterial efficiency, good biocompatibility, and low risk in antibiotics pollution; these advantages may be particularly helpful in preventing infections that involve medical devices.

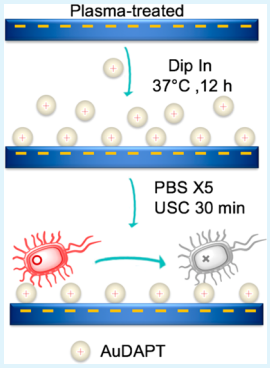

KEYWORDS: *nosocomial infections, gold nanoparticles, self-assembly, biocompatibility, antimicrobial*

1. INTRODUCTION

The rapid emergence of superbugs due to the abuse of antibiotics has become a public health crisis and led to worldwide panic. Infections caused by superbugs are especially severe in the hospital, which result in the continually growing number of deaths around the world.[1] Currently a large proportion of nosocomial (hospital- and clinic-based) infections are closely associated with medical devices such as ventilators, catheters, injectors, implantable scaffold devices, and so forth.[2] For the avoidance of these infections, the systematic use of antibiotics as the traditional measure would become useless and worsen the condition of drug resistance. Moreover, over the last 3 decades, no major new types of antibiotics have been developed to be approved for use in humans.[3] Even though several drugs have been recently proposed to treat multidrug resistance (MDR) Gram-positive bacteria,[4,5] none has been invented to treat MDR Gram-negative bacteria that is frequently involved in medical devices-associated infections. Developing a coating for medical devices against the threat of Gram-negative bacteria is thus urgently in need.

Coating the surface of biomedical devices with antimicrobial agents as a preventative way against nosocomial infections can provide an avenue for the prevention of infection because designing entirely novel antibiotics is extremely challenging.[2,6] For this purpose, a huge number of types of antibacterial coating with different compositions and fabrication strategies have emerged. However, almost all of them have severe limitations, such as poor biocompatibility, and the inability to eradicate MDR bacteria. For example, amphipathic polymers are widely applied to design antimicrobial coatings,[7] but because their antibacterial activity mainly relies on the strongly positively charged moieties, they thus are typically quite toxic to host cells.[7] The boom of nanotechnology has generated many antimicrobial nanomaterials.[8−11] Among them, silver-based nanomaterials have already gained popularity in many commercialized products. Unfortunately, their inherent adverse biological effects, due to the release of silver ion, restrict their further development in biomedical applications.[12,13] Among their well-known toxicity and side effects, a recent study shows that coating the catheter with Ag nanoparticles accelerated the coagulation of contacting blood.[14] Different from most other metal nanomaterials, gold nanoparticles (AuNPs) are relatively safe without appreciable toxicity, and they are not reported to release heavy metal ions in biological fluids that are common for many other heavy-metal-based nanomaterials. AuNPs are used in a broad range of applications, including photothermic therapy,[15] biochemical sensing, and drug development.[16,17]

Received: April 13, 2017
Accepted: June 5, 2017
Published: June 5, 2017

DOI: 10.1021/acsami.7b05230
ACS Appl. Mater. Interfaces 2017, 9, 21181−21189

However, AuNPs are not antimicrobial by themselves, so in most cases, AuNPs serve as carriers for known antibiotics to enhance their activity,[18,19] which can significantly attenuate toxicity and drug-resistance. Besides these inherent limitations on these antimicrobial agents, another tough issue is the difficulty in large-scale fabrication of nanoparticles on different solid surfaces. Current approaches based on layer-by-layer deposition,[20] chemical interaction, or nanolithography are often costly,[21] time-consuming, and substrate- or morphology-specific.[22] Given the two major limitations mentioned above, facile fabrication of nanoparticles to form coatings on the surface of medical devices against nosocomial infections without elevating the toxicity remains a great challenge.

We herein describe a facile and scalable strategy to prepare stable antimicrobial coatings by electrostatic self-assembling 4,6-diamino-2-pyrimidinethiol (DAPT, not antibacterial by itself)-conjugated AuNPs (AuDAPT) on the surfaces of a variety of medical devices. AuDAPT possesses a positively charged surface so that they should be easily and stably absorbed on negatively charged surfaces.[23] We previously reported that AuDAPT in aqueous solutions can kill MDR Gram-negative bacteria efficiently and induced drug resistance to a much-smaller degree than conventional antibiotics. Moreover, AuDAPT is nontoxic to normal cells.[23,24] In this study, we explore a universal method of fabricating AuDAPT on a variety of solid surfaces and investigate their antimicrobial performance via colony counting, optical density measurement, live−dead staining, and scanning electron microscopy. We also evaluate different parameters and conditions that influence the density and stability of AuDAPT immobilized on solid surfaces. In addition, we employ both in vitro and in vivo assays to evaluate the biocompatibility of AuDAPT-based coating, including their influences on cell viability, hemolysis, coagulation, and inflammation. We hope that our approach provides antimicrobial coating that exhibit robust antibacterial activity without compromised biocompatibility and further inspires the designing novel antimicrobial coating against superbug-related nosocomial infection.

2. MATERIALS AND METHODS

2.1. Materials. We purchased all chemicals from major suppliers such as Alfa Aesar and Sigma-Aldrich (ACS grade) unless otherwise noted. $HAuCl_4{\cdot}3H_2O$ (99.99%) is from Shangjuly Chemical Co., Ltd., China. Cell culture plates (polystyrene, PS) are from Corning Incorporated. Catheters (polyvinyl chloride, PVC−polydimethylsiloxane, PDMS) are from China Guangzhou MeCan Medical Equipment Co., Ltd. Injector (polypropylene, PP) and polyethylene (PE) films are from Shanghai Zhiyu Medical Equipment Co. Ltd. Silica glass slides (SiO_2) are from Jiangsu Huida medical instruments Co., Ltd., China. PDMS slices are prepared from SYLGARD 184 SILICONE ELASTOMER KIT (Dow Corning). We raised female BALB/c nude mice in a specific pathogen-free (SPF) environment (25−30 g, Beijing Vital River Laboratory Animal Technology Co., Ltd.; Beijing, China) and performed all care and handling of animals with the approval of Institutional Authority for Laboratory Animal Care of Institute of Process Engineering, Chinese Academy of Science. We received healthy human blood from The General Hospital of the People's Liberation Army (Beijing, China). We obtain *Escherichia coli* (*E. coli,* ATCC 11775), *Pseudomonas aeruginosa* (*P. aeruginosa*, ATCC 27853), *Klebsiella pneumoniae* (*K. pneumoniae,* ATCC 13883), and *S. aureus* (*S.aureus,* ATCC 6538P) from China General Microbiological Culture Collection Center and received clinical strains of MDR *E. coli* (BJ915), MDR *P. aeruginosa* (BJ915), and MDR *K. pneumoniae* (R12K2637) from Beijing Tian Tan Hospital.

2.2. Synthesize of AuDAPT. We synthesized AuDAPT as previous report with slight modifications.[23] Briefly, in a 100 mL round-bottom flask, we added a mixture of DAPT (10 mM, 40 μL of Tween-80 and 200 μL of acetic acid, dissolved in 10 mL of H_2O) to a solution of 10 mL of $HAuCl_4$ $3H_2O$ (10 mM). The mixture turned from yellow to orange and underwent further stirring for 5 min in an ice−water bath. We added the $NaBH_4$ solution (12 mg, 5 mL) drop-by-drop along with vigorous stirring. The stirring continued for another 1 h. We dialyzed the solution and sterilized it through a 0.22 μm filter (Millipore), and we stored the purified AuNPs at 4 °C for further use. We determine the concentration of AuDAPT with an inductively coupled plasma optical emission spectrometer (ICP-OES, PerkinElmer Optima 5300 V). We observed AuDAPT with a transmission electron microscope (TEM, FEI Tecnai G2 T20). The UV−vis spectrum is achieved with a UV2450 spectrophotometer (Shimadzu), and the ζ potential was collected with a Zetasizer (Malvern Zetasizer 3000HS and He/Ne laser at 632.8 nm at a scattering angle of 90 deg at 25 °C).

2.3. Fabrication and Characterization of DAPT- and AuDAPT-Based Coating on Different Substrates. We washed the surfaces of different substrates with deionized water (DI water) and dried them under a flowing stream of nitrogen. We treated these substrates with oxygen plasma for 4 min (PDC-MG, Chengdu Mingheng Technology Co., Ltd.) and soaked the oxidized substrates immediately into the solution of DAPT (10 mM, dissolved in 10 mL of H_2O by adding 200 μL of acetic acid)/AuDAPT for a defined time to allow coating formation. After soaking, we rinsed these substrates with water for 30 s and further washed them with phosphate-buffered saline (PBS) under ultrasound to remove the unbound AuDAPT. Unless specifically noted, the coating concentration of AuDAPT in this research is 0.6 mg/L. We collected the photos of AuDAPT-coated substrates with a Nikon D90 digital camera and recorded the absorbance of theses substrates with a UV2450 spectrophotometer. We measured the contact angle with a Kruss DSA-100 system and sterilized these substrates under UV light for 2 h for further experimentation.

We also fabricated flat gold surfaces directly coated with DAPT according to our previous procedure with slight modifications.[25] We first prepared gold-covered glass slides by evaporating titanium (5 nm) followed by gold (20−50 nm) onto glass coverslips. Afterward, we dipped the gold-coated coverslips into 10 mM DAPT dissolved in methyl alcohol for 12 h to form self-assembled monolayers. We washed these substrates with PBS 10 times and sterilized these substrates under UV light for 2 h for further analysis.

2.4. Calculating the Surface Density of Gold on AuDAPT-Based Coating. After the coatings formed, we dissolved the AuDAPT attached on the surfaces with chloroazotic acid and further diluted the solutions with 0.3% (vt %) HNO_3 solution to appropriate concentrations. We then measured the Au^{3+} concentration with ICP-OES to calculate the content of Au on the surface.

The leaching ratio of Au on different surfaces follows this formula:

$$\begin{aligned}\text{leaching ratio of Au (\%)} = {} & (\text{content of Au on treated samples} \\ & - \text{content of Au on untreated samples}) \\ & /(\text{content of Au on untreated samples}) \\ & \times 100\% \end{aligned} \quad (1)$$

2.5. Colony Assay. We adjusted the concentration of bacteria in Luria-Bertan (LB, Difco) medium to about 10^8 colony-forming units (CFU)/mL (correspondence to the $OD_{600\ nm}$ is 0.1 via a UV2450 spectrophotometer, Shimadzu); we then diluted the bacterial suspension to 10^5 CFU/mL by LB and added the diluted bacterial suspension (100 μL) onto untreated and AuDAPT-coated substrates. After incubation at 37 °C for 24 h, we collected the bacterial suspensions and diluted them to appropriate concentrations. We spread the diluted bacterial suspension on an agar plate (1.25% agar in LB) and counted the number of the CFUs after incubation for 24 h at 37 °C. We performed each colony assay test three times for consistency.

DOI: 10.1021/acsami.7b05230
ACS Appl. Mater. Interfaces 2017, 9, 21181−21189

2.6. Live–Dead Staining Assay for Bacteria. We seeded the bacteria suspensions (10^5 CFU/mL, 100 μL) on the untreated and AuDAPT-coated PS plates and incubated them at 37 °C. After 24 h of incubation on the surfaces of the PS plates, we washed them with PBS buffer three times and added a dye solution (5.01 μM of SYTO 9 and 30 μM of propidium iodide in PBS, Invitrogen) to image the viable bacteria at room temperature in the dark for 15 min. In this experiment, the propidium iodide stains dead bacteria by penetrating damaged cell membrane, and SYTO 9 stains all the bacteria. We used an oil-immersed 63× objective lens on a Zeiss LSM 5 DUO laser scanning confocal microscope (Germany) to image the stained bacterial cells. For all fluorescence images, the microscope settings including brightness, contrast, and exposure time were constant for comparison of the relative intensity of intracellular fluorescence.

2.7. Scanning Electron Microscope Imaging for Bacteria. To observe the *E. coli* via scanning electron microscopy (SEM) after incubating with AuDAPT-based coating, we incubated suspensions of *E. coli* (10^5 CFU/mL, 100 μL) on AuDAPT-coated and untreated PS plates at 37 °C for 4 h. We washed these plates three times with sterile PBS and fixed the bacteria by 2.5% glutaraldehyde in PBS for 2 h at 37 °C. We further dehydrated the fixed bacteria with ethanol solution with gradually increased concentration (25%, 50%, 75%, 80%, 90%, 95%, and 100% at 15 min each) and then performed platinum coating. We used a Hitachi S-4800 (Japan) field-emission scanning electron microscope to record SEM images.

2.8. Antibiofilm Activity Assay against *P. aeruginosa*. We evaluate the antibiofilm activity of AuDAPT-based coating with following static biofilm formation assay. Briefly, we add untreated and AuDAPT-coated PDMS discs (0.1 mm × 0.6 mm × 0.6 mm) to the suspension of *P. aeruginosa* at the log phase (10^8 CFU/mL in LB medium) and made sure that the AuDAPT-coated surfaces are facing the bacterial suspensions. We further incubated at 37 °C for 24 h to allow the formation of biofilm. Afterward, we rinsed with distilled water to remove the unattached bacteria and scraped the attached bacteria in the biofilms with cell scrapers (Corning). We then suspended the scraped bacteria into 200 μL of PBS and performed serial dilutions for colony assay.

2.9. Cell Culture and Toxicity Assays. We cultured human umbilical vein endothelial cell (HUVEC, ATCC), human aortic vascular smooth muscle cell (HAVSMC, ATCC), and human aortic fibroblasts (HAF, Science Cell) in Dulbecco's modified Eagle's medium (DMEM, Gibco) supplemented with 10% fetal bovine serum (FBS, Gibco). Cultured Raw264.7 (mouse monocyte macrophage) in DMEM supplemented with 10% inactivated FBS (heated in 57 °C for 30 min), glutamine (2 mM), and 1% penicillin–streptomycin were maintained at 37 °C in a humidified 5% CO_2 atmosphere.

We performed cell toxicity assay with both cell-counting kit (CCK8, DOJINDO, Japan) assays and morphology observation. Briefly, we seeded 100 μL suspensions that contain 5000 different cells in untreated and AuDAPT-coated 96 well plates and cultured them for 24 h at 37 °C. We replaced the medium with 200 μL of fresh media containing 20 μL of CCK8 solution and incubated them for 3 h. We measured the absorbance at 450 nm (A) using a microplate reader. We used the absorbance from the cells on untreated plates as a negative control (A_n) and set the blank control (A_b) by adding the same volume of the CCK8 solution into the untreated wells without cells. The calculation of cell viability follows the following equation:

$$\text{cell viability (\%)} = (A - A_b)/(A_n - A_b) \times 100\% \quad (2)$$

After incubation on untreated and AuDAPT-coated 96 well plates, we washed the cells attached to the surfaces with PBS buffer three times and then soaked them in the dye solution (5.01 μM of calcium green, Invitrogen) for 15 min in the dark at room temperature. We add a solution of 30 μM of propidium iodide (Invitrogen) in PBS for another incubation of 15 min, performed another three rounds of washing, and imaged the cells with a Leica microscope 6100A (Germany) to observe the morphology and density. For all fluorescence images, the microscope settings including brightness, contrast, and exposure time are constant for the comparison of the relative intensity of intracellular fluorescence.

2.10. Hemolysis Assay. We collected fresh human blood from healthy volunteers and diluted it to 4% (by volume) with PBS. We incubated 200 μL of diluted human blood on the surface of uncoated and AuDAPT-coated PS plates for 1 h at 37 °C to allow hemolysis to occur and then centrifuged the blood dilutions at 2200 rpm for 5 min. We then measured the optical density at 576 nm ($OD_{576\,nm}$) of supernatants from each sample to evaluate the hemoglobin release. In this assay, we use the diluted blood with 0.2% Triton-X as a positive control and used the diluted blood without any other treatment as a negative control. We calculated the hemolysis percentage with the following formula:

$$\begin{aligned}\text{hemolysis (\%)} = {} & (OD_{576\,nm} \text{ of the sample} \\ & - OD_{576\,nm} \text{ of the negative control}) \\ & /(OD_{576\,nm} \text{ of the positive control} \\ & - OD_{576\,nm} \text{ of the negative control}) \times 100\%\end{aligned} \quad (3)$$

We expressed the data as the mean and standard deviation of three replicates.

2.11. Thrombin Generation and Platelet Adhesion Assay. We added D-Phe-pro-arg-ANSNH (Haematologic Technologies), which yielded a fluorescent product when prothrombin activates into thrombin, to fresh PRP with a final concentration of 50 μM. We "recalcified" the mixtures by adding a $CaCl_2$ stock solution (0.5 M $CaCl_2$) to a final concentration of 10 mM $CaCl_2$ and then immediately transferred 100 μL of sample to untreated or AuDAPT-coated 96 well plates at room temperature. We measured the fluorescence at 470 nm as the result of D-phe-pro-arg-ANSNH hydrolysis every minute with a microplate reader. We performed thrombin generation assays in triplicate and calculated the mean thrombin-generation curves using Thrombinoscope software (Thrombinoscope BV).

We placed fresh PRP obtained from healthy donors on untreated or AuDAPT-coated PS plates and incubated at 37 °C for 1 h. After incubation, we fixed and dehydrated the platelets with the same procedure as that of *E. coli* for SEM imaging.

2.12. Inflammation Assay. To analyze the in vitro inflammation, we seeded Raw 264.7 onto untreated and AuDAPT-coated 96 well plates. After culturing these cells for 7 days, we counted and stimulated these cells with lipopolysaccharide (100 ng/mL) and then collected the supernatants for the analysis of tumor necrosis factor α (TNF-α) and interleukin (IL-6) using standard enzyme enzyme-linked immunosorbent assay (ELISA) protocols. For measuring IL-1β, we stimulated cells with ATP (5 mM) for 1 h.

We performed in vivo inflammation generation assay by measuring the content of TNF-α, IL-6, and IL-1β in mice with standard ELISA kits (Invitrogen). Before measuring, we prepared untreated AuDAPT-coated small PDMS discs and subcutaneously implanted them into the backs of healthy mice. After 1 or 2 weeks of implantation, we collected mouse blood and used the blood from mice without any treatment as a blank control.

2.13. Hematoxylin and Eosin Staining. After the subcutaneous implantation of AuDAPT-coated PDMS discs (0.1 mm × 0.6 mm × 0.6 mm) into the backs of healthy mice for 1 or 2 weeks, we euthanized mice by CO_2 asphyxiation. We excised tissues surrounding the PDMS discs and fixed them in zinc fixative overnight. We then embedded them in paraffin wax. For each sample, we cut and mounted 6 μm sections onto slides for histological staining. We examined the inflammatory response after 1 or 2 weeks by staining with hematoxylin and eosin (H&E) staining, which stains nuclei dark purple or blue to black and cell cytoplasm pink. We recorded the images with a Leica DMI6000 B inverted microscope (Germany).

2.14. Statistical Analysis. We performed all of the statistical analyses using SPSS 13.0 software (American), and we analyzed the differences between different groups by a one-way analysis of variance (ANOVA) followed by Tukey multiple comparisons. We expressed error bars as standard deviation from the mean (mean ± SD).

DOI: 10.1021/acsami.7b05230
ACS Appl. Mater. Interfaces 2017, 9, 21181–21189

3. RESULT AND DISCUSSIONS

3.1. Synthesis and Characterization of AuDAPT. We prepared AuDAPT by reducing tetrachloroauric acid by sodium borohydride in the presence of DAPT in aqueous solutions. These NPs exhibit maximum absorbance at around 530 nm. TEM images indicated that the diameter of spherical AuDAPT is around 3 nm. In addition, both the TEM image and dynamic light scattering (DLS) measurement confirm that the as-prepared AuDAPT have a narrow size distribution (Figure S1). AuDAPT are positively charged (ζ potential = +17 ± 1.26 mV) in aqueous solutions at pH 7, which is in accordance with previous reports about using pyridine or aromatic amine to generate positive surface for AuNPs.[8,23,26,27] As a result, AuDAPT are well-dispersed in aqueous solutions by electrostatic repulsion and could easily adsorb on negatively charged surfaces.

3.2. Characterization of AuDAPT-Based Coating on Different Substrates. To test our hypothesis, we first obtained a negatively charged surface by treating cell-culture plates with oxygen plasma, which would introduce chemical groups with negative surface potential (φ_{surf}) values on the surface.[28] These oxygen-plasma-treated cell culture plates have no antibacterial activity by themselves, but a step of incubation with AuDAPT allows them to have antibacterial capabilities (Scheme 1).[29] We washed the AuDAPT-treated plates in ultrasound with PBS for 2 h to remove unbound NPs. These NPs-coated substrates are transparent with a brown hue and exhibit a maximum absorbance at 530 nm ($A_{530\ nm}$) as a result of the successful modification of AuDAPT. The amount of Au that have been irreversibly deposited is 1.109 ± 0.021 $\mu g/cm^2$, as determined by inductively coupled plasma optical emission spectrometer, using untreated plates as a control (Figure 1a). This experiment also confirms that plasma oxidation is necessary for fabricating AuDAPT-based coating. The electrostatic interactions between the negatively charged substrates and the AuDAPT prevent the stabilized particles from being washed away by PBS under ultrasound.[28,29] Without plasma oxidation, much less AuDAPT adsorbs via nonspecific interaction and can be easily washed away. The successful modification of the substrate with AuDAPT can also increase the hydrophilicity of the surface (Figure 1b).

Scheme 1. Electrostatic Self-Assembly of AuDAPT-Based Antimicrobial Coating on a Solid Surface

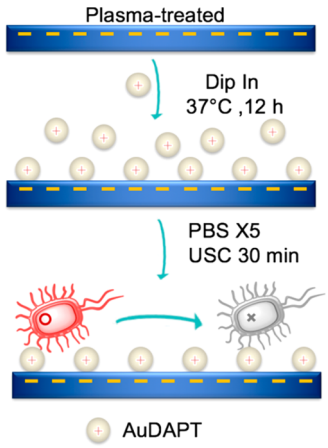

Next, we used PS plates as a model system to investigate the parameters that influence the amount and stability of AuDAPT that absorb on the surface. We used the $A_{530\ nm}$ value as the main criteria by which to evaluate the parameters because it is proportional to the density of nanoparticles.[30] By increasing the incubation time, ionic strength, or incubation concentrations of AuDAPT, we can assemble a larger amount of AuDAPT on the surface of the solid substrates (Figure 1c–e), which is in accordance with a previous report.[31] In the absence of NaCl, the maximum coverage of Au we can obtain on a 96 well plate is 1.109 ± 0.021 $\mu g/cm^2$. Using ICP-OES, the $A_{530\ nm}$ values increase with the amount of AuDAPT on the surfaces (Figure S2); thus, in the following study, we represent the coverages of AuDAPT with the $A_{530\ nm}$ value of the AuDAPT-coated PS plates. We also show that AuDAPT can modify a variety of substrates typically used for manufacturing medical devices, including PS, PVC, PP, PE, and glasses, which are frequently used for medical devices (Figure 1f).

3.3. Antibacterial Behavior on the Surface of AuDAPT-Coated Substrates. To investigate the antibacterial activities AuDAPT-coated substrates, we incubated the bacterial suspensions (10^5 CFU/mL and 100 μL) of *E. coli or S. aureus* on AuDAPT-coated substrates for 8 or 24 h. The values of optical density at 600 nm ($OD_{600\ nm}$) indicate that the coating can efficiently inhibit the growth of *E. coli* (Figure 2a). However, AuDAPT-coated substrates cannot inhibit the growth of *S. aureus* (Figure S3), which coincides the activity of AuDAPT in aqueous solutions and is possibly due to the thick peptidoglycan of Gram-positive bacteria.[11] We further determined the number of viable *E. coli* after 24 h of incubation by plating and counting colony-forming units (CFU), and we found that no colony can form from the suspension (undiluted) on AuDAPT-coated substrates, whereas a large number of colonies can form from the diluted suspension (by 10^7) on an untreated surface (Figure S4). We further confirm the results with live–dead staining: live bacteria (green) are visible on control substrates (Figure 2b) but not visible on AuDAPT-coated substrates (Figure 2c). In addition, SEM images also show that *E. coli* cultured on AuDAPT-coated substrates (Figure 2d) exhibit membrane disruptions and undergo morphological changes compared to those on untreated substrates (Figure 2e); such results are consistent with our previous reports of the antibacterial activity of AuDAPT in aqueous solutions, in which AuDAPT eradicate bacteria by disrupting their membranes.[23,24] These results also agree with other studies that indicate that disrupting the membrane is closely associated the antibacterial activities of AuNPs.[32,33] As a comparison, we also incubated plasma-treated plates with DAPT (10 mM) under the same procedure as that of AuDAPT, and these substrates cannot inhibit the growth of *E. coli*. In addition, coating planar surface of gold with DAPT cannot result in antibacterial surfaces (Figure S5) either, which means that conjugating DAPT on AuNPs is essential for the antibacterial activity. To further test whether or not incubation of the AuDAPT-coated substrates with bacterial suspensions results in the release of AuDAPT into the solution, we calculated the content of Au on the cell culture plates before and after bacterial incubation based on ICP-OES measurement. We do not detect measurable decrease for the content of Au on the coating after incubating (Table S1), which coincides previous report in which electrostatic self-assembly can stabilize AuNPs during cell culturing.[28] The result indicates that the immobilized AuDAPT, instead of AuDAPT released from the substrates, are responsible for killing the bacteria by interacting and disrupting their membrane.

DOI: 10.1021/acsami.7b05230
ACS Appl. Mater. Interfaces 2017, 9, 21181–21189

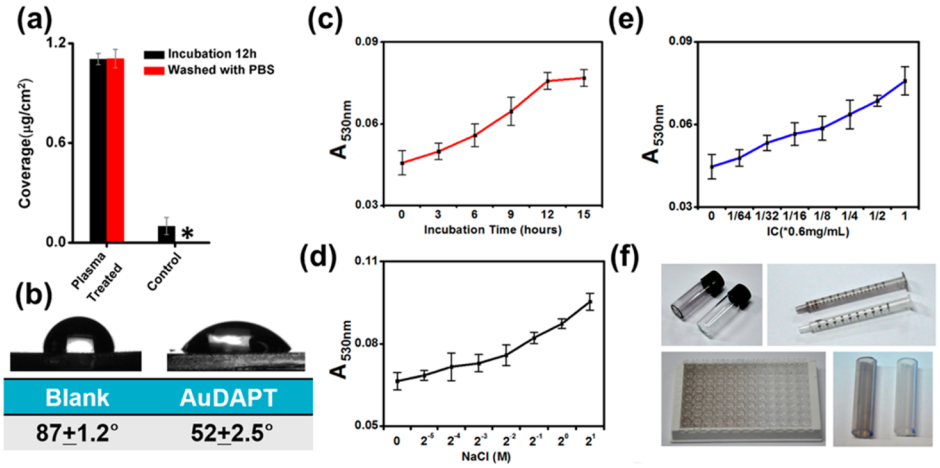

Figure 1. Characterization of AuDAPT-based coating on different substrates. (a) Coverage of Au atoms on a PS plate with or without plasma (Control) treatment by ICP-OES (n = 3, mean ± SD). (b) Contact angle of AuDAPT-coated and untreated (blank) PS plates (n = 3, mean ± SD). (c–e) Dependence of the absorbance for AuDAPT-coated PS plates at 530 nm on the incubation time, incubation concentration, and salt concentration (n = 3, mean ± SD). (f) Photos of AuDAPT-coated glasses, injector, 96 well plate, and catheter. Coating with AuDAPT induced a brown color change in proportion to the coverage of AuDAPT.

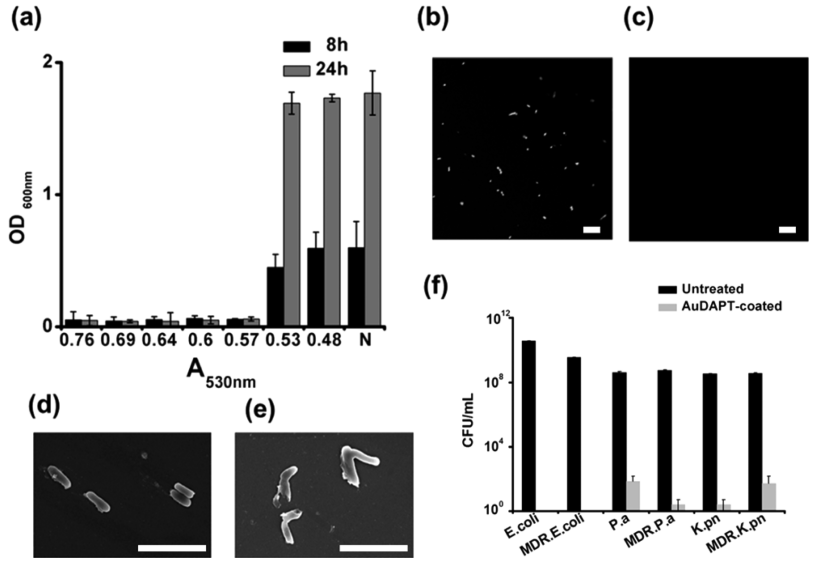

Figure 2. Antibacterial behavior of AuDAPT-coated substrates. (a) $OD_{600\ nm}$ of *E. coli* suspension incubated with AuDAPT-coated PS plates with different coverage (represented with the $A_{530\ nm}$ value of AuDAPT-coated PS plates) for 8 or 24 h, where N is untreated (n = 3, mean ± SD) (b) Live–dead staining of *E. coli* after culturing on untreated culturing plates for 24 h. (c). Live–dead staining of *E. coli* after culturing on AuDAPT-coated cell culturing plates for 24 h. Scale bar for panels b and c: 20 μm. (d) SEM image of *E. coli* that was incubated with untreated PS plates for 4 h. (e) SEM image of *E. coli* that was incubated with AuDAPT-coated PS plates for 4 h. Scale bars for panels d and e: 4 μm. (f) Colony assays of different bacteria cultured on AuDAPT-coated or untreated PS plates (n = 3, mean ± SD).

3.4. Activity of AuDAPT-Based Antimicrobial Coating against Different Bacteria. We further tested the antibacterial activities of AuDAPT-based coating against three representative types of Gram-negative bacteria, including *E. coli*, *P. aeruginosa*, and *K. pneumoniae*, as well as their multidrug-resistant mutants, which frequently appear in biomedical device-associated, nosocomial infections.[2,34,35] After incubating the bacterial suspensions with AuDAPT-coated PS plates with different surface coverage, we measured the $OD_{600\ nm}$ after 8 and 24 h to confirm that coatings with highest coverage (1.109 ± 0.021 $\mu g/cm^2$) can totally inhibit the growth of different Gram-negative bacteria (Figure S6). In addition, we perform plating and colony counting assay after 24 h of incubation, which indicates that NPs-based coatings at maximum coverage can efficiently kill different Gram-negative bacteria (Figure 2f).

3.5. Antibiofilm Activity of AuDAPT-Based Coating. The formation of bacteria-based biofilm on medical devices is a serious problem in nosocomial infections because bacteria are very hard to eradicate once biofilm form.[36] Thus, we evaluate our coating against biofilm formation of *P. aeruginosa* by static biofilm formation assay[37] and found that the AuDAPT-coated surface (1.109 ± 0.021 $\mu g/cm^2$) can reduce the development of biofilm for *P. aeruginosa* by 99% compared to the untreated surfaces (Figure S7). Such an effect is comparable to several coatings based on the release of metal ions[38,39] and further ensures the potential application of our approach.

3.6. Stability and Universality of This Coating Strategy on Antibacterial Efficiency. To ensure that the antibacterial ability of coatings is broadly applicable to typical substrates used in medical devices, we fabricated AuDAPT-

DOI: 10.1021/acsami.7b05230
ACS Appl. Mater. Interfaces 2017, 9, 21181–21189

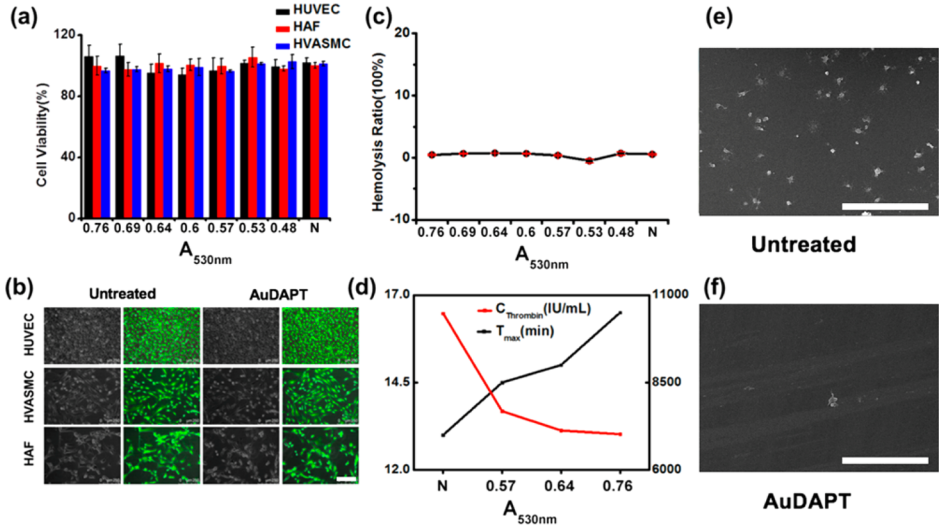

Figure 3. Biocompatibility of AuDAPT-coated surface. (a) Cell viability of HUVEC, HAF, and HVASMC after culturing on AuDAPT-coated PS plates with different coverage (n = 3, mean ± SD). (b) Cell morphology of HUVEC, HAF, and HVASMC after culturing on AuDAPT-coated and untreated PS plates. Scale bar: 250 μm. (c) Hemolysis ratio of AuDAPT-coated PS plates with different coverage (n = 3, mean ± SD). N: untreated. (d) Maximum thrombin generation and T_{max} on AuDAPT-coated PS plates with different coverage. N: untreated. (e) SEM image of platelet adhesion on untreated PS plates. (f) SEM image of platelet adhesion AuDAPT-coated PS plates. Scale bar for panels e and f: 30 μm.

based coatings on different materials, including PVC, PP, PE, PDMS, and SiO_2, with the same procedures as those on PS plates. We incubated suspensions (10^5 CFU/mL and 100 μL) of *E. coli* with these coatings on different materials for 24 h and then implemented colony-counting assays. None of the suspensions (undiluted) that were incubated with different substrates formed more than a single colony on agar plates (Table S2). These results confirm that we can modify a variety of substrates with AuDAPT as a surface coating to yield a material with desired bactericidal activity because the plasma treatment on many kinds of different substrates can endow them with negative φ_{surf} values for further electrostatic self-assembly.[28−31]

The stability of antibacterial coating is very important for long-term and constant antibacterial activity of medical devices. To test the stability of such coating in our study, we stored AuDAPT-coated substrates at different medium for 1 month and carried out plating and colony-counting assays to show that these coatings retain their antibacterial as well as freshly prepared ones (Table S3). To test the leaching from AuDAPT-based coating, we measured the content of Au before and after incubation with different medium with ICP-OES via dissolving AuDAPT-based coating with chloroazotic acid; thus, the leaching of either AuDAPT or Au ions from the surfaces would result in the change of the Au content measured by ICP-OES. As a result, we do not find significant leaching of Au from the surfaces that incubated with different medium compared to untreated surfaces (Figure S8), which further confirms that neither AuDAPT nor Au ions can be released from AuDAPT-based coating after storage and that the immobilized AuNPs are responsible for the antibacterial activities. Using a similar procedure, we also confirmed that neither Au ions nor AuDAPT can leach from multiple surfaces after storage (Figure S8). These results further imply the stability of our coating.

Although the employment of gold may increase the cost compared to that of silver- or polymer-based coatings,[7,12,29] when considering our method, we do not rely on bulk equipment, and the coverage of Au in our coating is extremely low (~1 μg/cm^2). In addition, the noble Au on the coating is very stable and recyclable because it does not leach after incubating with bacteria. Thus, the cost of our method is negligible compared to the treatment cost for infections and has much fewer environmental problems in comparison with those that rely on the release of metal ions (Table S4). Another key impact of the stability of the substrate is that none of the antibiotic components can easily enter into the environment to freely diffuse and thus are unlikely to cause secondary contamination and potentially breed drug resistance, such as silver-based NPs that unavoidably leach Ag ions.[12,40] Both the stability and universality endow this coating strategy with great potential for medical-device-related applications.

3.7. Cytotoxicity on AuDAPT-Coated Surfaces. Compared with other heavy-metal-based NPs, a major advance of using AuNPs instead of other nanomaterials as antibacterial coating is the lower toxicity of AuNPs; thus, we examined the toxicity of AuDAPT-based coating on several different cell lines including HUVEC, HAVSMC, and HAF. We seed suspensions of different cells on AuDAPT-coated and untreated PS plates. After 48 h of culturing, we tested the cell viability with a commercial kit (CCK8). The viability of all cells cultured on AuDAPT-coated PS plates exhibits no statistical differences compared to those cultured on untreated cell culture plates (Figure 3a). In addition, we observed these cells after culturing them on AuDAPT-coated PS plates at maximum coverage via a Leica fluorescence microscope in both the phase-contrast and the fluorescent modes. All of these cells show similar attachment and survival as well as density to those cultured on untreated plates and exhibit typical morphology (Figure 3b). These results suggest that antibacterial coating obtained from AuDAPT is not cytotoxic to normal mammalian cells.

3.8. Blood Compatibility on AuDAPT-Coated Surfaces. As antibacterial coating for medical devices, blood compatibility is certainly very important because many medical devices would necessarily interact with human blood. Hemolysis is a major issue that prevents many exogenous materials from becoming useful for medical devices. We thus examine the hemolysis effect of AuDAPT-based coating by measuring the release of hemoglobin after incubating fresh blood from healthy human

DOI: 10.1021/acsami.7b05230
ACS Appl. Mater. Interfaces 2017, 9, 21181−21189

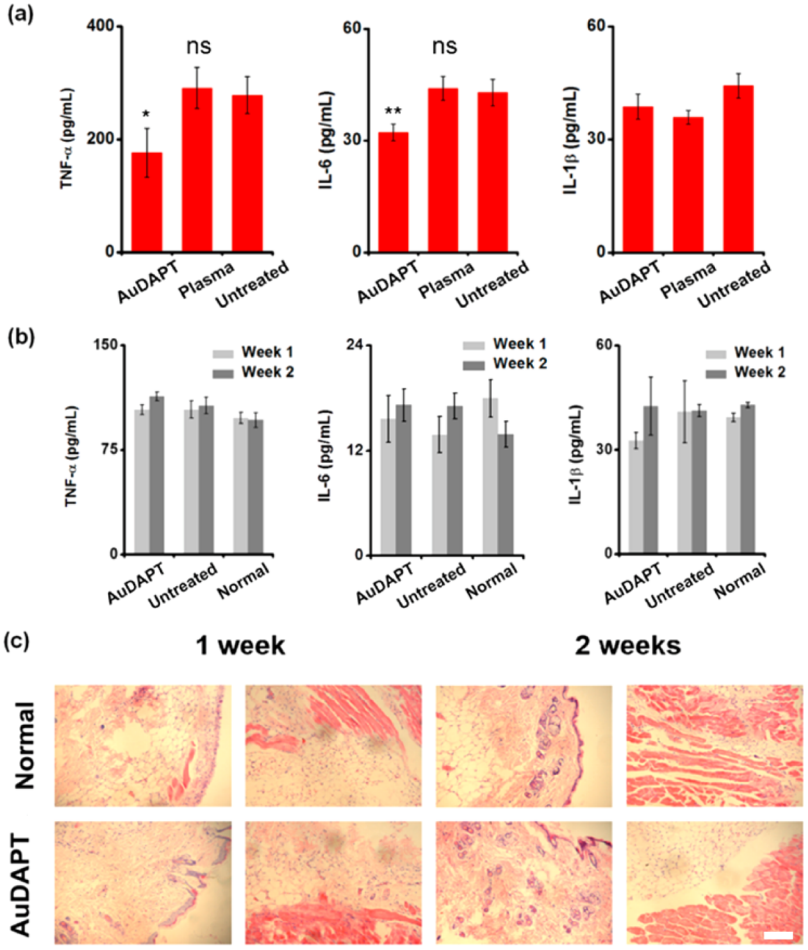

Figure 4. In vitro and in vivo inflammatory responses to AuDAPT-coated substrates. (a) Detection of TNF-α, IL-6, and IL-1β in Raw264.7 cultured on AuDAPT-coated, plasma-treated, and untreated PS plates (n = 6, mean ± SD). Results from t-test: *, $P < 0.05$; **,$P < 0.01$; ns, not significant. (b) Detection of TNF-α, IL-6, and IL-1β level in normal mice and mice blood after hypodermic implantation of untreated and AuDAPT-coated PDMS discs (0.1 mm × 0.6 mm × 0.6 mm); n = 6, mean ± SD. (c) H&E staining images for skin and subcutaneous tissues of normal and mice with hypodermic implantation of AuDAPT-coated PDMS discs (0.1 mm × 0.6 mm × 0.6 mm). Scale bar: 200 μm.

on AuDAPT-coated plates. AuDAPT-coated substrates would not induce any hemolysis regardless of coverage (Figure 3c).

We next evaluate the risk of these AuDAP-coated substrates for thrombosis, which is another common side effect for medical devices. Previous studies indicate that the development of improved coating for medical devices should be antibacterial and nonthrombogenic, but some commercialized silver-NPs-based coating can accelerate the coagulation of contacting blood or induce thrombosis.[14,41] Compared to AgNPs, our previous study shows that dispersed AuDAPT in aqueous solutions exhibit antithrombotic functions without increasing bleeding risk;[42] thus, in this study, we investigate the anticoagulant effect of AuDAPT-based coating by measuring the generation of thrombin. We incubate fresh platelet-rich plasma (PRP) from healthy donors on PS plates with different coverage of AuDAPT to perform the thrombin generation assays. AuDAPT-based coating can both prolong the lag time (T_{max}) and decrease the peak concentration of active thrombin compared to the control group, thus demonstrating the antithrombotic effect. The antithrombotic effect positively correlates to the density of AuDAPT in the coating (Figures 3d and S9), which is also in line with our expectations. Moreover, SEM images indicate that AuDAPT-coated PS plates induce less platelet adhesion compared to uncoated PS plates (Figure 3e,f). The decreased platelet adhesion is most likely due to the fact that AuDAPT can reduce the activation and aggregation of platelet, which is closely involved in the attachment of platelet.[42] This result further confirms the anticoagulant effect of AuDAPT-based coating. All the aforementioned results ensure adequate blood compatibility for AuDAPT-based antimicrobial coatings.

3.9. In Vitro and in Vivo Inflammatory Responses to AuDAPT-Coated Substrates. We further access the inflammatory responses of AuDAPT-based coating by evaluating the levels of three pro-inflammatory cytokines, TNF-α, and IL-6 and IL-1β, which are important for assessing the innate immune response. Even though many kinds of antibacterial coatings are available, few reports have studied the possible adverse innate immune effect, which is a serious problem for these coatings for medical application.[43] After culturing Raw 264.7 (a cell line often used to study inflammatory responses in vitro) on AuDAPT-coated and untreated PS plates, we measured the expressions of the three cytokines with standard ELISA kits. We observed no statistically significant difference in IL-1β expression between Raw 264.7 cultured on AuDAPT-coated and that on untreated PS plates. Moreover, AuDAPT can slightly reduce the immune response by reducing the expression of TNF-α and IL-6 (Figure 4a). This result is very

DOI: 10.1021/acsami.7b05230
ACS Appl. Mater. Interfaces 2017, 9, 21181−21189

useful because some studies also indicate AuNPs can increase or decrease pro-inflammatory cytokines, but the effect is related to the size and surface properties of AuNPs, and the mechanism needs further study.[44,45] After confirming that AuDAPT-based coating would not induce enhanced immune response for macrophage in vitro, we further employed an in vivo study to access the possible immune inflammatory effect of using AuDAPT-coated substrates as implanted devices. We implant small PDMS discs with or without AuDAPT-based coating into the back of healthy mice and assayed the expression of pro-inflammatory cytokines including TNF-α, IL-6, and IL-1β in their blood. Neither AuDAPT-coated nor untreated PDMS discs could significantly alter the expression of these cytokines compared to normal mice after 1 or 2 weeks post-implantation (Figure 4b). In addition, H&E staining images from the tissue that are in contact with the PDMS also reveal that AuDAPT-based coating would not induce inflammatory responses compared to normal mice (Figure 4c). All of these results suggest the potential of using AuDAPT to the fabrication of antimicrobial coating for implantable devices.

4. CONCLUSIONS

We have provided a facile strategy for the manufacturing of a highly stable, AuNP-based antibacterial coating that exhibits outstanding antibacterial activity against Gram-negative bacteria on a variety of surfaces made from PS, PVC, PP, PE, PDMS, and SiO_2. Comprehensive evaluation of the biocompatibility indicates that such materials are safe for medical devices. Our methods can alleviate the severity of infection on implantable medical devices as well as wearable electronics. Because the active ingredient (AuDAPT) does not leach into the environment, no active antibiotics will likely enter into the environment to result in secondary contaminations or potentially induce the emergence of superbugs.

■ ASSOCIATED CONTENT

Supporting Information

The Supporting Information is available free of charge on the ACS Publications website at DOI: 10.1021/acsami.7b05230.

Figures showing AuDAPT characterization, the relationship between Au coverage and A_{530nm} values, optical density, colony assays, optical density, number of CFUs on biofilms, leaching of Au, and thrombin generation. Tables showing AuDAPT coverage, antibacterial efficiency, and comparison of approach costs. (PDF)

■ AUTHOR INFORMATION

Corresponding Author

*E-mail: xingyujiang@nanoctr.cn.

ORCID

Xuefeng Guo: 0000-0001-5723-8528

Xingyu Jiang: 0000-0002-5008-4703

Present Address

⊥Wenwen Chen, Guangdong Key Laboratory for Biomedical Measurements and Ultrasound Imaging, School of Biomedical Engineering Shenzhen University, Shenzhen 518060, China

Notes

The authors declare no competing financial interest.

■ ACKNOWLEDGMENTS

We thank the Ministry of Science and Technology of China (grant no. 2013YQ190467), the Chinese Academy of Sciences (grant no. XDA09030305), and the National Science Foundation of China (grant nos. 81361140345, 51373043, and 21535001) for financial support.

■ REFERENCES

(1) Rosenthal, V. D.; Maki, D. G.; Mehta, Y.; Leblebicioglu, H.; Memish, Z. A.; Al-Mousa, H. H.; Balkhy, H.; Hu, B. J.; Alvarez-Moreno, C.; Medeiros, E. A.; Apisarnthanarak, A.; Raka, L.; Cuellar, L. E.; Ahmed, A.; Navoa-Ng, J. A.; El-Kholy, A. A.; Kanj, S. S.; Bat-Erdene, I.; Duszynska, W.; Van Truong, N.; Pazmino, L. N.; See-Lum, L. C.; Fernandez-Hidalgo, R.; Di-Silvestre, G.; Zand, F.; Hlinkova, S.; Belskiy, V.; Al-Rahma, H.; Luque-Torres, M. T.; Bayraktar, N.; Mitrev, Z.; Gurskis, V.; Fisher, D.; Abu-Khader, I. B.; Berechid, K.; Rodriguez-Sanchez, A.; Horhat, F. G.; Requejo-Pino, O.; Hadjieva, N.; Ben-Jaballah, N.; Garcia-Mayorca, E.; Kushner-Davalos, L.; Pasic, S.; Pedrozo-Ortiz, L. E.; Apostolopoulou, E.; Mejia, N.; Gamar-Elanbya, M. O.; Jayatilleke, K.; de Lourdes-Duenas, M.; Aguirre-Avalos, G. International Nosocomial Infection Control Consortiu (Inicc) Report, Data Summary of 43 Countries for 2007−2012. Device-Associated Module. *Am. J. Infect. Control.* **2014**, *42*, 942−956.

(2) Noimark, S.; Dunnill, C. W.; Wilson, M.; Parkin, I. P. The Role of Surfaces in Catheter-Associated Infections. *Chem. Soc. Rev.* **2009**, *38*, 3435−3448.

(3) Piddock, L. J. V. The Crisis of No New Antibiotics-What Is the Way Forward? *Lancet Infect. Dis.* **2012**, *12*, 249−253.

(4) Levy, S. B.; Marshall, B. Antibacterial Resistance Worldwide: Causes, Challenges and Responses. *Nat. Med.* **2004**, *10*, S122−S129.

(5) Lehar, S. M.; Pillow, T.; Xu, M.; Staben, L.; Kajihara, K. K.; Vandlen, R.; DePalatis, L.; Raab, H.; Hazenbos, W. L.; Morisaki, J. H.; Kim, J.; Park, S.; Darwish, M.; Lee, B. C.; Hernandez, H.; Loyet, K. M.; Lupardus, P.; Fong, R. N.; Yan, D. H.; Chalouni, C. C.; Luis, E.; Khalfin, Y.; Plise, E.; Cheong, J. C.; Lyssikatos, J. P.; Strandh, M.; Koefoed, K.; Andersen, P. S.; Flygare, J. A.; Wah Tan, M; Brown, E. J.; Mariathasan, S. Novel Antibody-Antibiotic Conjugate Eliminates Intracellular S. Aureus. *Nature* **2015**, *527*, 323−328.

(6) Li, W.; Dong, K.; Ren, J.; Qu, X. A Beta-Lactamase-Imprinted Responsive Hydrogel for the Treatment of Antibiotic-Resistant Bacteria. *Angew. Chem., Int. Ed.* **2016**, *55*, 8049−8053.

(7) Yang, C.; Ding, X.; Ono, R. J.; Lee, H.; Hsu, L. Y.; Tong, Y. W.; Hedrick, J.; Yang, Y. Y. Brush-Like Polycarbonates Containing Dopamine, Cations, and Peg Providing a Broad-Spectrum, Antibacterial, and Antifouling Surface Via One-Step Coating. *Adv. Mater.* **2014**, *26*, 7346−7351.

(8) Feng, Y.; Chen, W. W.; Jia, Y. X.; Tian, Y.; Zhao, Y. Y.; Long, F.; Rui, Y. K.; Jiang, X. Y. N-Heterocyclic Molecule-Capped Gold Nanoparticles as Effective Antibiotics against Multi-Drug Resistant Bacteria. *Nanoscale* **2016**, *8*, 13223−13227.

(9) Zhao, Y. Y.; Ye, C. J.; Liu, W. W.; Chen, R.; Jiang, X. Y. Tuning the Composition of AuPt Bimetallic Nanoparticles for Antibacterial Application. *Angew. Chem., Int. Ed.* **2014**, *53*, 8127−8131.

(10) Huh, A. J.; Kwon, Y. J. "Nanoantibiotics": A New Paradigm for Treating Infectious Diseases Using Nanomaterials in the Antibiotics Resistant Era. *J. Controlled Release* **2011**, *156*, 128−145.

(11) Zhao, Y. Y.; Chen, Z. L.; Chen, Y. F.; Xu, J.; Li, J. H.; Jiang, X. Y. Synergy of Non-Antibiotic Drugs and Pyrimidinethiol on Gold Nanoparticles against Superbugs. *J. Am. Chem. Soc.* **2013**, *135*, 12940−12943.

(12) Chernousova, S.; Epple, M. Silver as Antibacterial Agent: Ion, Nanoparticle, and Metal. *Angew. Chem., Int. Ed.* **2013**, *52*, 1636−1653.

(13) Wang, Z. Z.; Dong, K.; Liu, Z.; Zhang, Y.; Chen, Z. W.; Sun, H. J.; Ren, J. S.; Qu, X. G. Activation of Biologically Relevant Levels of Reactive Oxygen Species by Au/G-C3n4 Hybrid Nanozyme for Bacteria Killing and Wound Disinfection. *Biomaterials* **2017**, *113*, 145−157.

(14) Stevens, K. N. J.; Crespo-Biel, O.; van den Bosch, E. E. M.; Dias, A. A.; Knetsch, M. L. W.; Aldenhoff, Y. B. J.; van der Veen, F. H.; Maessen, J. G.; Stobberingh, E. E.; Koole, L. H. The Relationship between the Antimicrobial Effect of Catheter Coatings Containing Silver Nanoparticles and the Coagulation of Contacting Blood. *Biomaterials* **2009**, *30*, 3682−3690.
(15) Rengan, A. K.; Bukhari, A. B.; Pradhan, A.; Malhotra, R.; Banerjee, R.; Srivastava, R.; De, A. In Vivo Analysis of Biodegradable Liposome Gold Nanoparticles as Efficient Agents for Photothermal Therapy of Cancer. *Nano Lett.* **2015**, *15*, 842−848.
(16) Zheng, W. S.; Li, H.; Chen, W. W.; Ji, J.; Jiang, X. Y. Recyclable Colorimetric Detection of Trivalent Cations in Aqueous Media Using Zwitterionic Gold Nanoparticles. *Anal. Chem.* **2016**, *88*, 4140−4146.
(17) Zhao, Y. Y.; Wang, Z.; Zhang, W.; Jiang, X. Y. Adsorbed Tween 80 Is Unique in Its Ability to Improve the Stability of Gold Nanoparticles in Solutions of Biomolecules. *Nanoscale* **2010**, *2*, 2114−2119.
(18) Chamundeeswari, M.; Sobhana, S. S. L.; Jacob, J. P.; Kumar, M. G.; Devi, M. P.; Sastry, T. P.; Mandal, A. B. Preparation, Characterization and Evaluation of a Biopolymeric Gold Nanocomposite with Antimicrobial Activity. *Biotechnol. Appl. Biochem.* **2010**, *55*, 29−35.
(19) Pissuwan, D.; Cortie, C. H.; Valenzuela, S. M.; Cortie, M. B. Functionalised Gold Nanoparticles for Controlling Pathogenic Bacteria. *Trends Biotechnol.* **2010**, *28*, 207−213.
(20) Lee, D.; Cohen, R. E.; Rubner, M. F. Antibacterial Properties of Ag Nanoparticle Loaded Multilayers and Formation of Magnetically Directed Antibacterial Microparticles. *Langmuir* **2005**, *21*, 9651−9659.
(21) Jain, P.; Pradeep, T. Potential of Silver Nanoparticle-Coated Polyurethane Foam as an Antibacterial Water Filter. *Biotechnol. Bioeng.* **2005**, *90*, 59−63.
(22) Haynes, C. L.; Van Duyne, R. P. Nanosphere Lithography: A Versatile Nanofabrication Tool for Studies of Size-Dependent Nanoparticle Optics. *J. Phys. Chem. B* **2001**, *105*, 5599−5611.
(23) Zhao, Y. Y.; Tian, Y.; Cui, Y.; Liu, W. W.; Ma, W. S.; Jiang, X. Y. Small Molecule-Capped Gold Nanoparticles as Potent Antibacterial Agents That Target Gram-Negative Bacteria. *J. Am. Chem. Soc.* **2010**, *132*, 12349−12356.
(24) Cui, Y.; Zhao, Y. Y.; Tian, Y.; Zhang, W.; Lu, X. Y.; Jiang, X. Y. The Molecular Mechanism of Action of Bactericidal Gold Nanoparticles on Escherichia Coli. *Biomaterials* **2012**, *33*, 2327−2333.
(25) Li, Y.; Yuan, B.; Ji, H.; Han, D.; Chen, S. Q.; Tian, F.; Jiang, X. Y. A Method for Patterning Multiple Types of Cells by Using Electrochemical Desorption of Self-Assembled Monolayers within Microfluidic Channels. *Angew. Chem., Int. Ed.* **2007**, *46*, 1094−1096.
(26) Gandubert, V. J.; Lennox, R. B. Assessment of 4-(Dimethylamino)Pyridine as a Capping Agent for Gold Nanoparticles. *Langmuir* **2005**, *21*, 6532−6539.
(27) Shiigi, H.; Yamamoto, Y.; Yoshi, N.; Nakao, H.; Nagaoka, T. One-Step Preparation of Positively-Charged Gold Nanoraspberry. *Chem. Commun.* **2006**, 4288−4290.
(28) Tang, R.; Moyano, D. F.; Subramani, C.; Yan, B.; Jeoung, E.; Tonga, G. Y.; Duncan, B.; Yeh, Y. C.; Jiang, Z. W.; Kim, C.; Rotello, V. M. Rapid Coating of Surfaces with Functionalized Nanoparticles for Regulation of Cell Behavior. *Adv. Mater.* **2014**, *26*, 3310−3314.
(29) Huda, S.; Smoukov, S. K.; Nakanishi, H.; Kowalczyk, B.; Bishop, K.; Grzybowski, B. A. Antibacterial Nanoparticle Monolayers Prepared on Chemically Inert Surfaces by Cooperative Electrostatic Adsorption (CELA). *ACS Appl. Mater. Interfaces* **2010**, *2*, 1206−1210.
(30) Kalsin, A. M.; Kowalczyk, B.; Smoukov, S. K.; Klajn, R.; Grzybowski, B. A. Ionic-Like Behavior of Oppositely Charged Nanoparticles. *J. Am. Chem. Soc.* **2006**, *128*, 15046−15047.
(31) Winkler, K.; Paszewski, M.; Kalwarczyk, T.; Kalwarczyk, E.; Wojciechowski, T.; Gorecka, E.; Pociecha, D.; Holyst, R.; Fialkowski, M. Ionic Strength-Controlled Deposition of Charged Nanoparticles on a Solid Substrate. *J. Phys. Chem. C* **2011**, *115*, 19096−19103.
(32) Hayden, S. C.; Zhao, G. X.; Saha, K.; Phillips, R. L.; Li, X. N.; Miranda, O. R.; Rotello, V. M.; El-Sayed, M. A.; Schmidt-Krey, I.; Bunz, U. H. F. Aggregation and Interaction of Cationic Nanoparticles on Bacterial Surfaces. *J. Am. Chem. Soc.* **2012**, *134*, 6920−6923.
(33) Gifford, J. C.; Bresee, J.; Carter, C. J.; Wang, G. K.; Melander, R. J.; Melander, C.; Feldheim, D. L. Thiol-Modified Gold Nanoparticles for the Inhibition of Mycobacterium Smegmatis. *Chem. Commun.* **2014**, *50*, 15860−15863.
(34) Maki, D. G.; Tambyah, P. A. Engineering out the Risk for Infection with Urinary Catheters. *Emerg. Infect. Dis.* **2001**, *7*, 342−347.
(35) Paterson, D. L.; Ko, W. C.; Von Gottberg, A.; Mohapatra, S.; Casellas, J. M.; Goossens, H.; Mulazimoglu, L.; Trenholme, G.; Klugman, K. P.; Bonomo, R. A.; Rice, L. B.; Wagener, M. M.; McCormack, J. G.; Yu, V. L. Antibiotic Therapy for Klebsiella Pneumoniae Bacteremia: Implications of Production of Extended-Spectrum Beta-Lactamases. *Clin. Infect. Dis.* **2004**, *39*, 31−7.
(36) Davies, D. Understanding Biofilm Resistance to Antibacterial Agents. *Nat. Rev. Drug Discovery* **2003**, *2*, 114−122.
(37) Natan, M.; Edin, F.; Perkas, N.; Yacobi, G.; Perelshtein, I.; Segal, E.; Homsy, A.; Laux, E.; Keppner, H.; Rask-Andersen, H.; Gedanken, A.; Banin, E. Two Are Better Than One: Combining Zno and Mgf2 Nanoparticles Reduces Streptococcus Pneumoniae and Staphylococcus Aureus Biofilm Formation on Cochlear Implants. *Adv. Funct. Mater.* **2016**, *26*, 2473−2481.
(38) Tran, P. L.; Hammond, A. A.; Mosley, T.; Cortez, J.; Gray, T.; Colmer-Hamood, J. A.; Shashtri, M.; Spallholz, J. E.; Hamood, A. N.; Reid, T. W. Organoselenium Coating on Cellulose Inhibits the Formation of Biofilms by Pseudomonas Aeruginosa and Staphylococcus Aureus. *Appl. Environ. Microb.* **2009**, *75*, 3586−3592.
(39) Roe, D.; Karandikar, B.; Bonn-Savage, N.; Gibbins, B.; Roullet, J. B. Antimicrobial Surface Functionalization of Plastic Catheters by Silver Nanoparticles. *J. Antimicrob. Chemother.* **2008**, *61*, 869−876.
(40) Xiu, Z. M.; Zhang, Q. B.; Puppala, H. L.; Colvin, V. L.; Alvarez, P. J. J. Negligible Particle-Specific Antibacterial Activity of Silver Nanoparticles. *Nano Lett.* **2012**, *12*, 4271−4275.
(41) Smock, K. J.; Schmidt, R. L.; Hadlock, G.; Stoddard, G.; Grainger, D. W.; Munger, M. A. Assessment of Orally Dosed Commercial Silver Nanoparticles on Human Ex Vivo Platelet Aggregation. *Nanotoxicology* **2014**, *8*, 328−333.
(42) Tian, Y.; Zhao, Y. Y.; Zheng, W. F.; Zhang, W.; Jiang, X. Y. Antithrombotic Functions of Small Molecule-Capped Gold Nanoparticles. *Nanoscale* **2014**, *6*, 8543−8550.
(43) Taheri, S.; Cavallaro, A.; Christo, S. N.; Smith, L. E.; Majewski, P.; Barton, M.; Hayball, J. D.; Vasilev, K. Substrate Independent Silver Nanoparticle Based Antibacterial Coatings. *Biomaterials* **2014**, *35*, 4601−4609.
(44) Khan, H. A.; Abdelhalim, M. A.; Alhomida, A. S.; Al Ayed, M. S. Transient Increase in Il-1beta, Il-6 and Tnf-Alpha Gene Expression in Rat Liver Exposed to Gold Nanoparticles. *GMR, Genet. Mol. Res.* **2013**, *12*, 5851−5857.
(45) Sumbayev, V. V.; Yasinska, I. M.; Garcia, C. P.; Gilliland, D.; Lall, G. S.; Gibbs, B. F.; Bonsall, D. R.; Varani, L.; Rossi, F.; Calzolai, L. Gold Nanoparticles Downregulate Interleukin-1beta-Induced Pro-Inflammatory Responses. *Small* **2013**, *9*, 472−477.

DOI: 10.1021/acsami.7b05230
ACS Appl. Mater. Interfaces 2017, 9, 21181−21189